High-power, high repetition-rate, green-pumped, picosecond LBO optical parametric oscillator

Florian Kienle,[1,*] Peh Siong Teh,[1] Dejiao Lin,[1] Shaif-ul Alam,[1] Jonathan H. V. Price,[1] D. C. Hanna,[1] David J. Richardson,[1] and David P. Shepherd[1]

[1]*Optoelectronics Research Centre, University of Southampton, Highfield, Southampton, SO17 1BJ, UK*
[*]*flk@orc.soton.ac.uk*

Abstract: We report on a picosecond, green-pumped, lithium triborate optical parametric oscillator with record-high output power. It was synchronously pumped by a frequency-doubled (530 nm), pulse-compressed (4.4 ps), high-repetition-rate (230 MHz), fiber-amplified gain-switched laser diode. For a pump power of 17 W, a maximum signal and idler power of 3.7 W and 1.8 W was obtained from the optical parametric oscillator. A signal pulse duration of ~3.2 ps was measured and wide tunability from 651 nm to 1040 nm for the signal and from 1081 nm to 2851 nm for the idler was achieved.

OCIS codes: (190.0190) Nonlinear optics; (190.4970) Parametric oscillators and amplifiers; (140.7090) Ultrafast lasers; (140.3515) Lasers, frequency doubled; (060.2320) Fiber optics amplifiers and oscillators; (320.5520) Pulse compression.

References and links

1. P. J. Campagnola and L. M. Loew, "Second-harmonic imaging microscopy for visualizing biomolecular arrays in cells, tissues and organisms," Nat. Biotechnol. **21**(11), 1356–1360 (2003).
2. W. R. Zipfel, R. M. Williams, R. Christie, A. Y. Nikitin, B. T. Hyman, and W. W. Webb, "Live tissue intrinsic emission microscopy using multiphoton-excited native fluorescence and second harmonic generation," Proc. Natl. Acad. Sci. U.S.A. **100**(12), 7075–7080 (2003).
3. C. W. Freudiger, W. Min, B. G. Saar, S. Lu, G. R. Holtom, C. He, J. C. Tsai, J. X. Kang, and X. S. Xie, "Label-free biomedical imaging with high sensitivity by stimulated Raman scattering microscopy," Science **322**(5909), 1857–1861 (2008).
4. C. L. Evans, E. O. Potma, M. Puoris'haag, D. Côté, C. P. Lin, and X. S. Xie, "Chemical imaging of tissue in vivo with video-rate coherent anti-Stokes Raman scattering microscopy," Proc. Natl. Acad. Sci. U.S.A. **102**(46), 16807–16812 (2005).
5. C. L. Evans and X. S. Xie, "Coherent anti-stokes Raman scattering microscopy: chemical imaging for biology and medicine," Annu. Rev. Anal. Chem. **1**(1), 883–909 (2008).
6. C. Cleff, J. Epping, P. Gross, and C. Fallnich, "Femtosecond OPO based on LBO pumped by a frequency-doubled Yb-fiber laser-amplifier system for CARS spectroscopy," Appl. Phys. B **103**(4), 795–800 (2011).
7. K. Kieu, B. G. Saar, G. R. Holtom, X. S. Xie, and F. W. Wise, "High-power picosecond fiber source for coherent Raman microscopy," Opt. Lett. **34**(13), 2051–2053 (2009).
8. S. D. Butterworth, S. Girard, and D. C. Hanna, "High-power, broadly tunable all-solid-state synchronously pumped lithium triborate optical parametric oscillator," J. Opt. Soc. Am. B **12**(11), 2158–2167 (1995).
9. M. Jurna, J. P. Korterik, H. L. Offerhaus, and C. Otto, "Noncritical phase-matched lithium triborate optical parametric oscillator for high resolution coherent anti-Stokes Raman scattering spectroscopy and microscopy," Appl. Phys. Lett. **89**(25), 251116 (2006).
10. J. D. Kafka, M. L. Watts, and J. W. Pieterse, "Synchronously pumped optical parametric oscillators with LiB3O5," J. Opt. Soc. Am. B **12**(11), 2147–2157 (1995).
11. T. W. Tukker, C. Otto, and J. Greve, "Design, optimization, and characterization of a narrow-bandwidth optical parametric oscillator," J. Opt. Soc. Am. B **16**(1), 90–95 (1999).
12. A. Ashkin, G. D. Boyd, J. M. Dziedzic, R. G. Smith, A. A. Ballman, J. J. Levinstein, and K. Nassau, "Optically-induced refracive index inhomogeneities in $LiNbO_3$ and $LiTaO_3$," Appl. Phys. Lett. **9**(1), 72–74 (1966).
13. Y. Furukawa, K. Kitamura, A. Alexandrovski, R. K. Route, M. M. Fejer, and G. Foulon, "Green-induced infrared absorption in MgO doped $LiNbO_3$," Appl. Phys. Lett. **78**(14), 1970–1972 (2001).
14. F. Kienle, D. Lin, S. U. Alam, H. S. S. Hung, C. B. E. Gawith, H. E. Major, D. J. Richardson, and D. P. Shepherd, "Green-pumped, picosecond MgO:PPLN optical parametric oscillator," J. Opt. Soc. Am. B **29**(1), 144–152 (2012).
15. S.-W. Chu, T.-M. Liu, C.-K. Sun, C.-Y. Lin, and H.-J. Tsai, "Real-time second-harmonic-generation microscopy based on a 2-GHz repetition rate Ti:sapphire laser," Opt. Express **11**(8), 933–938 (2003).

#158496 - $15.00 USD Received 21 Nov 2011; revised 29 Dec 2011; accepted 30 Dec 2011; published 13 Mar 2012

16. K. König, T. W. Becker, P. Fischer, I. Riemann, and K. J. Halbhuber, "Pulse-length dependence of cellular response to intense near-infrared laser pulses in multiphoton microscopes," Opt. Lett. **24**(2), 113–115 (1999).
17. K. K. Chen, J. H. V. Price, S.-U. Alam, J. R. Hayes, D. J. Lin, A. Malinowski, and D. J. Richardson, "Polarisation maintaining 100W Yb-fiber MOPA producing μJ pulses tunable in duration from 1 to 21 ps," Opt. Express **18**(14), 14385–14394 (2010).
18. K. Kato, "Temperature-tuned 90° phase-matching properties of LiB3O5," IEEE J. Quantum Electron. **30**(12), 2950–2952 (1994).
19. J. W. Nicholson, A. D. Yablon, S. Ramachandran, and S. Ghalmi, "Spatially and spectrally resolved imaging of modal content in large-mode-area fibers," Opt. Express **16**(10), 7233–7243 (2008).
20. F. Kienle, K. K. Chen, S.-U. Alam, C. B. E. Gawith, J. I. Mackenzie, D. C. Hanna, D. J. Richardson, and D. P. Shepherd, "High-power, variable repetition rate, picosecond optical parametric oscillator pumped by an amplified gain-switched diode," Opt. Express **18**(8), 7602–7610 (2010).

1. Introduction

There is a growing demand for tunable femto- or picosecond pulses in the visible and the near-IR spectral region. Such sources are required for a number of applications, especially in the area of multi-photon microscopy due to advances in techniques such as second-harmonic generation [1, 2], stimulated Raman scattering (SRS) [3] and coherent anti-Stokes Raman scattering (CARS) [4, 5]. Ti:Sapphire lasers are the most commonly used laser for such applications, but recently frequency-doubled, mode-locked, Yb-doped fiber lasers and/or master-oscillator power-amplifier (MOPA) systems have been used to pump optical parametric oscillators (OPO) as a robust, compact and power-scalable alternative [6, 7]. In particular, synchronously pumped OPOs are ideal for CARS and SRS in that two temporally synchronous pulses at different and tunable wavelengths are produced.

Lithium triborate (LBO) is the most prevalent nonlinear crystal for green-pumped OPOs [6–11], because it does not suffer from detrimental effects such as photo-refraction or green-induced IR absorption as in lithium-niobate-based materials [12–14], for example. Also, LBO has a damage threshold of > 10 GW/cm^2, a transparency range from 160 nm to 3200 nm and a nonlinear coefficient of d_{eff} = 1.17 pm/V for a type I interaction ($e \rightarrow o + o$). Tukker *et al.* reported the highest signal output power of 1.6 W from an LBO OPO (no idler output) with an input pump power of 5.6 W generated in a frequency-doubled, 50 ps Nd:YLF laser [11]. The signal was tunable from 744 nm to 930 nm. Using fiber-based MOPA pump sources, femtosecond [6] and picosecond [7] systems have been demonstrated that are tunable over ~200 nm in the near-IR, but at the < 1 W level.

Here, we demonstrate the first green-pumped picosecond LBO OPO using a frequency-doubled, pulse-compressed, Yb:fiber-amplified, gain-switched laser diode MOPA pump source with broadly tunable, high-power output well-suited to CARS and SRS microscopy applications with biological samples [3, 5]. Furthermore, we note that high repetition rates reaching into the GHz regime are preferred in some circumstances in order to avoid nonlinearly induced damage of such biological samples while maintaining a good signal-to-noise ratio [15, 16].

2. Pump source experimental setup

A schematic diagram of the 1060 nm pump source is shown in Fig. 1 and is similar to the system reported in [17]. Modifications included the addition of pre-amplifier 1 (to increase the seed power for pre-amplifier 2) and the use of a 3.5 m-long, end-capped and angle-cleaved Yb:fiber (PLMA-YDF-25/250-VIII, Nufern, USA) with a 25 μm core and a 250 μm inner cladding diameter (for improved pump absorption). At the output of the final amplifier, a maximum power of ~90 W was measured for ~160 W of pump power. This was reduced to ~75 W after a free-space optical isolator with typical M^2-values of < 1.3. The repetition rate for the experiments described here was set to 230 MHz as an example of relatively high repetition rate operation while ensuring sufficient peak intensities for the subsequent nonlinear frequency conversion processes.

#158496 - $15.00 USD Received 21 Nov 2011; revised 29 Dec 2011; accepted 30 Dec 2011; published 13 Mar 2012

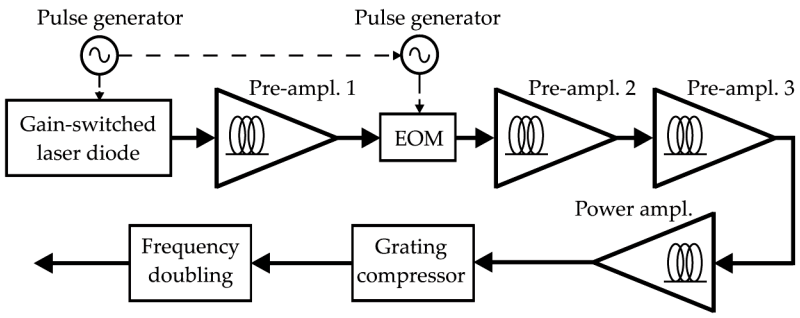

Fig. 1. Schematic diagram of the frequency-doubled, pulse-compressed, Yb:fiber-amplified, gain-switched laser diode MOPA pump system. EOM = electro-optic modulator.

The spectrum broadened with increasing power due to self-phase modulation and this additional bandwidth allowed for subsequent pulse compression. The grating compressor used a fused silica transmission grating (Ibsen Photonics A/S, Denmark) with 1250 lines/mm and a high diffraction efficiency of > 90%. The grating was used in a four-pass Littrow configuration. This led to a simplified alignment and increased throughput efficiency. Anti-reflection-coated (AR) right-angle prisms were used for horizontal and vertical translation of the beam and the overall throughput efficiency of the compressor was 70%. By changing the optical path length in the compressor, a minimum output pulse duration of 4.4 ps was experimentally achieved. With a spectral FWHM of 0.67 nm, the corresponding time-bandwidth product was calculated to be 0.79.

Frequency doubling was performed in a 20 × 3 × 3 mm^3 LBO crystal (Eksma Optics, Lithuania). The crystal was AR-coated for 1060 nm and 530 nm and was operated in a type I non-critical phase-matching (NCPM) arrangement at a temperature of 155 ºC. The fundamental 1060 nm beam was focused with a lens to a $1/e^2$-waist diameter of ~55 µm inside the crystal, which was experimentally determined to yield the best conversion efficiency of ~60% at high power. Up to ~25 W of 530 nm green light was generated from 42 W of fundamental power. The residual fundamental light was filtered with two dichroic mirrors. The pulse duration was not measured due to the lack of appropriate pulse diagnostics for the green spectral region.

3. Optical parametric oscillator experimental setup

The OPO resonator is shown in Fig. 2. It consisted of an LBO nonlinear crystal, two spherical curved mirrors (CM) and two plane mirrors, one of which acted as the signal output coupler (OC), in a bow-tie, ring cavity arrangement. The LBO crystal (Eksma Optics, Lithuania) used in the OPO had dimensions of 50 × 5 × 5 mm^3 and was AR-coated for the pump (530 nm) and the signal (650 nm to 1060 nm). It was cut for a type I NCPM interaction along the *x*-axis ($e \rightarrow o + o$, θ = 90º, φ = 0º). The extraordinary polarization of the pump in the *y*-axis was adjusted with a half-wave plate to achieve birefringent phase-matching (signal and idler polarized in the *z*-axis). The crystal was held in an oven with a resolution of 0.1 ºC for temperature tuning. Since LBO features only a moderate nonlinear coefficient, a long crystal was chosen to reduce the threshold, which was acceptable since the temporal walk-off of the pump and signal pulses along the crystal was only ~1.6 ps.

#158496 - $15.00 USD Received 21 Nov 2011; revised 29 Dec 2011; accepted 30 Dec 2011; published 13 Mar 2012

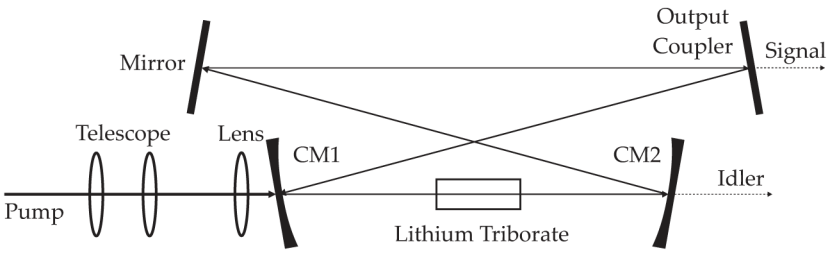

Fig. 2. Schematic diagram of the synchronously pumped, bow-tie LBO OPO ring resonator. CM1, CM2 = curved mirrors.

The resonator optical path length was set to 1.3 m to match the pump source repetition rate of 230 MHz. The resonator was modeled using the ABCD matrix formalism and with the constraints of the 1.3 m resonator length and the –250 mm CM radius of curvature, signal waist radii of 73.4 µm and 73.1 µm were calculated in the *x*-plane (resonator plane) and *y*-plane (perpendicular to resonator plane), respectively. This corresponds to a focusing parameter (crystal length divided by confocal parameter) of $\xi_s = 0.78$, which means that the signal focusing was somewhat weaker than the optimal confocal focusing ($\xi_s = 1$). The slightly elliptical signal beam was due to the astigmatism introduced by the curved mirrors associated with the bow-tie resonator angle of 14.9°. To obtain good mode matching of signal and pump in the crystal center, a two-lens telescope for beam expansion and an $f = 250$ mm focusing lens were used to generate a measured pump beam waist radius of 72 µm × 61 µm (parallel and perpendicular to the resonator plane, respectively). All mirrors were highly transmissive at the pump wavelength of 530 nm ($T > 99\%$) and over the idler tuning range ($T > 90\%$ from 1.2 µm to 3 µm) and highly reflective (HR) in the signal tuning range ($R > 99.5\%$ from 650 nm to 1090 nm), except for the OC, which had a signal transmission of $T_{OC} = 10\%$.

4. Experiments and results

Phase-matching and wavelength tuning of the OPO was achieved by temperature and cavity length tuning. Figure 3 shows the tuning curve with the two characteristic signal and idler branches leading to two possible pairs of signal and idler wavelengths at temperatures between ~100 ºC and ~160 ° C. Because of the variation in group delay between different (phase-matched) signal wavelengths and the required pulse synchronism of pump and signal, the OPO operated first on one and then the other signal as the cavity length was scanned [10]. A signal (idler) tuning range from 651 nm to 1040 nm (1081 nm to 2851 nm) was measured. The theoretical LBO tuning curve was derived from the temperature-dependent Sellmeier equation as given in [18].

#158496 - $15.00 USD Received 21 Nov 2011; revised 29 Dec 2011; accepted 30 Dec 2011; published 13 Mar 2012

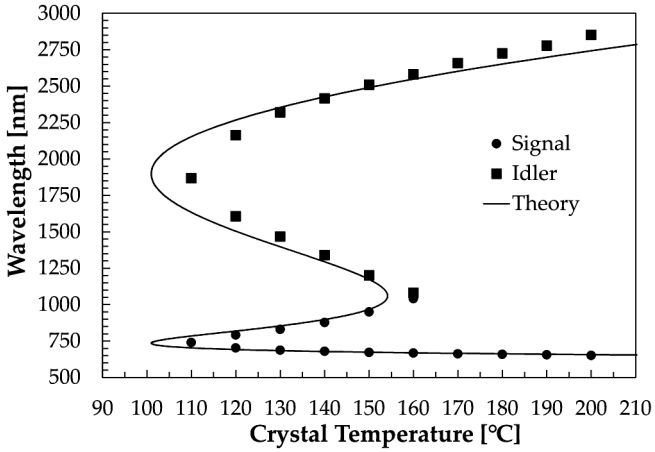

Fig. 3. Temperature tuning results with the theoretical tuning curve derived from the temperature-dependent Sellmeier equation of LBO [18].

The signal and idler power levels over the entire tuning range and for a constant pump power of 17 W at 530 nm are plotted in Fig. 4, where the OPO cavity length was adjusted to yield maximum output powers. The figure shows that up to 3.7 W of signal (740 nm) and 1.8 W of idler (1.34 μm) were produced. The idler power dropped rapidly towards zero for wavelengths > 2 μm due to the combination of the decreasing quantum ratio λ_p/λ_i, the absorption in an idler collimation lens as well as a pump/idler filter used after CM2 (non-transmissive substrates for mid-IR). The signal power drop at the short wavelength side was caused by the mirror coating characteristics. The power decrease and the characteristically unstable performance near degeneracy were due to some idler feedback and the associated doubly resonant oscillation.

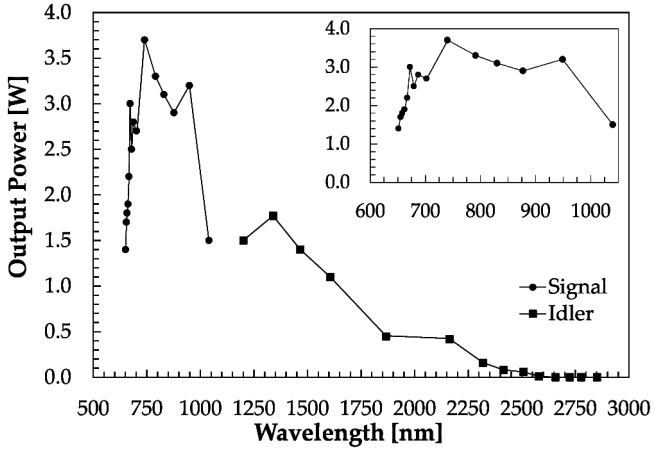

Fig. 4. Output power versus tuning wavelength with 17 W of pump power and a T_{OC} = 10% signal OC. The inset shows the signal tuning region for more clarity. The solid lines are a guide to the eye.

The highest combined output power was obtained at a temperature of 140 ° C (signal at 877 nm and idler at 1.34 μm) and the output powers and pump depletion as a function of the input pump power are shown in Fig. 5. A signal power of 2.5 W and an idler power of 1.7 W were measured for 17 W of pump power. The slope efficiencies were ~17% and ~11% for signal and idler, respectively. The oscillation threshold was 1.3 W and the pump depletion reached ~45%. Using this pump depletion, the pump and signal powers above, the quantum ratio λ_p/λ_s and the 10% output coupling, a signal round-trip loss of ε_s = 8.5% was calculated

#158496 - $15.00 USD Received 21 Nov 2011; revised 29 Dec 2011; accepted 30 Dec 2011; published 13 Mar 2012

[11], which was attributed to the LBO coating losses (~1.7% per surface), some transmission loss of the imperfect HR mirror coatings (T ~0.1% per mirror at 877 nm) and other scattering losses. Since at the time of the experiments, we had only one OC with T_{OC} = 10% at hand, an optimization of the output power by finding the optimum output coupling transmission was not possible and will be addressed in the future. The available pump power is high enough to accept a higher threshold when using an OC with a higher transmission, which would increase the slope efficiency and eventually the maximum signal and idler power.

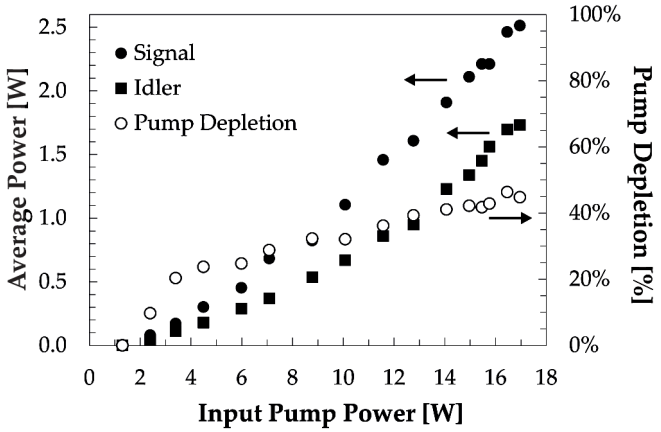

Fig. 5. Output power and pump depletion versus pump power at a signal wavelength of 877 nm (idler at 1.34 µm) and with a 10% signal OC.

The pulse duration of the signal pulses at 740 nm was measured with an intensity autocorrelator. Since the pump source exhibited temporal and spatial instabilities (discussed below), autocorrelation traces of consecutive measurements were not consistent and the FWHM values varied somewhat. The average FWHM width from several traces was approximately 4.5 ps corresponding to a pulse duration of 3.2 ps, if a Gaussian pulse profile is assumed.

Reliable M^2-measurements of the OPO output beams and measurements of the signal spectrum were complicated by a spatial beam instability that was already existent on the input pump beam. The slow scanning time of the optical spectrum analyzer in combination with the unstable signal power input to the device led to a strongly modulated spectrum. Similarly, the beam incident on the M^2-beam profiler drifted too quickly compared to the acquisition time of the device. Beam pointing instabilities from modal interference [19] due to some higher-order mode content as well as thermal and mechanical instabilities of the final amplifier fiber that were augmented by the long optical path length of 10.5 m between the MOPA output and the OPO input (long compressor, frequency-doubling stage) were the main reasons for this. Truly single-mode operation could be obtained by using a fiber with a smaller core diameter, which would however increase the fiber nonlinearities. Improved thermal management of the final amplifier is also likely to reduce the instability. Indeed, recent work in our group using the same fiber type but improved heat sinking and optimal mode excitation showed that M^2-values of < 1.1 are obtainable, i.e. essentially fundamental mode operation. Under these conditions the beam pointing instabilities were reduced to a minimum and we plan to build on the current OPO results in the near future and add results from spectral, temporal as well as beam quality measurements to the experimental data given in this publication.

To increase the attraction for nonlinear microscopy even further and simultaneously allow a much more compact OPO cavity, the system could be operated at higher repetition rates. For this particular setup, a four-times higher repetition rate of 920 MHz is readily feasible. For the same average power, this would lead to a four-times reduction in peak power and hence an increase of the OPO threshold to ~5 W. Therefore, as long as we can generate sufficient green light several times above this threshold, GHz operation is feasible.

#158496 - $15.00 USD Received 21 Nov 2011; revised 29 Dec 2011; accepted 30 Dec 2011; published 13 Mar 2012

5. Summary

In summary, we have, to the best of our knowledge, demonstrated record-high output powers of up to 3.7 W from an attractive green-pumped LBO OPO. The system, tunable from ~0.65 µm to ~2.85 µm, was operated at a repetition rate of 230 MHz and a signal pulse duration of 3.2 ps. The gain-switched laser diode and Yb-doped fiber MOPA pump source has the potential to be operated between 100 MHz and 1 GHz [20], which in combination with the few-picosecond pulse duration and the near-IR tunability of the OPO represents an attractive source for nonlinear microscopy. In future experiments, we plan to complement the initial results given here with spectral, temporal and beam quality measurements.

Acknowledgments

Dr. J. H. V. Price is supported by a Royal Academy of Engineering / EPSRC (UK) Research Fellowship. F. Kienle acknowledges the support of an EPSRC studentship.

#158496 - $15.00 USD Received 21 Nov 2011; revised 29 Dec 2011; accepted 30 Dec 2011; published 13 Mar 2012